applied sciences

MDPI

Review

Glucose Isomerase: Functions, Structures, and Applications

Ki Hyun Nam [1,2]

[1] Department of Life Science, Pohang University of Science and Technology, Pohang 37673, Korea; structures@postech.ac.kr
[2] POSTECH Biotech Center, Pohang University of Science and Technology, Pohang 37673, Korea

Abstract: Glucose isomerase (GI, also known as xylose isomerase) reversibly isomerizes D-glucose and D-xylose to D-fructose and D-xylulose, respectively. GI plays an important role in sugar metabolism, fulfilling nutritional requirements in bacteria. In addition, GI is an important industrial enzyme for the production of high-fructose corn syrup and bioethanol. This review introduces the functions, structure, and applications of GI, in addition to presenting updated information on the characteristics of newly discovered GIs and structural information regarding the metal-binding active site of GI and its interaction with the inhibitor xylitol. This review provides an overview of recent advancements in the characterization and engineering of GI, as well as its industrial applications, and will help to guide future research in this field.

Keywords: glucose isomerase; xylose isomerase; high-fructose corn syrup; HFCS; bioethanol; structure

check for updates

Citation: Nam, K.H. Glucose Isomerase: Functions, Structures, and Applications. *Appl. Sci.* **2022**, *12*, 428. https://doi.org/10.3390/app12010428

Academic Editor: Hidehiko Hirakawa

Received: 30 October 2021
Accepted: 3 December 2021
Published: 3 January 2022

Publisher's Note: MDPI stays neutral with regard to jurisdictional claims in published maps and institutional affiliations.

1. Introduction

Glucose isomerase (GI, EC 5.3.1.5; also known as D-xylose ketol isomerase, xylose isomerase (XI), xylose ketoisomerase, and xylose ketol-isomerase) is widely distributed in bacteria, actinomycetes, fungi, and plants [1,2]. This enzyme is an intramolecular oxidoreductase that can interconvert aldoses and ketoses. GI occupies a pivotal position with respect to its physiological role and commercial applications [3]. It is one of the three most commonly produced industrial enzymes, along with amylase and protease [2,3]. In particular, this enzyme is extensively used in the industrial production of high-fructose corn syrup (HFCS) [2]. Moreover, the bioconversion of xylose to ethanol by GI is important for the production of bioethanol from hemicellulose [4]. In this review, I introduce the molecular function, structural characteristics, and industrial applications of GI and describe the recent crystallographic results related to GI structure.

2. Function

2.1. Substrate Specificity

Glucose/xylose isomerase (GI/XI) is known to catalyze the reversible isomerization of D-glucose and D-xylose to D-fructose and D-xylulose, respectively (Figure 1).

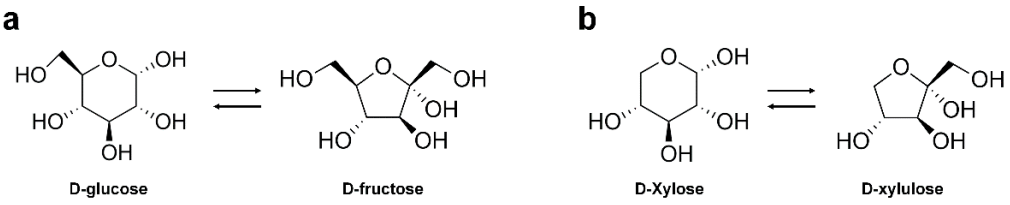

Figure 1. Catalytic reaction of glucose isomerase. Reversible isomerization between (**a**) D-glucose and D-fructose, and (**b**) D-xylose and D-xylulose.

In addition to its natural substrates, GI can isomerize various pentoses, hexoses, sugar alcohols, and sugar phosphates. It exhibits activity against a broad spectrum of sugar

substrates, including D-ribose [5], L-rhamnulose [6], L-arabinose [7], and D-allose [8], although the substrate specificity of GIs can vary depending on the source strain or organism [1]. For example, GI from *Streptomyces griseofuscus* S-41 shows isomerase activity on D-glucose (activity 100%) and D-xylose (287%) as well as on D-ribose (20%) [5]. The GI from *Streptomyces rubiginosus* exhibits activity on L-arabinose, in addition to D-glucose and D-xylose [7]. L-arabinose is widely used in food products with a low glycemic index, and in pharmaceutical and chemical industries [9]. The commercially available immobilized GI from *Streptomyces murinus* (SmGI) has previously been used to produce L-rhamnulose (6-deoxy-L-sorbose) from 300 g L^{-1} L-rhamnose in a packed-bed reactor, with a 45% conversion yield [6]. L-rhamnulose plays an important role in sugar metabolism and has wide applications in the flavor industry [6,10]. Furthermore, SmGI has been employed to produce D-allose from D-allulose in a packed bed reactor [11]. At the optimal conditions of pH 8.0 and 60 °C, SmGI produced an average of 150 g/L D-allose over 20 days from 500 g/L D-allulose as the substrate (productivity of 36 g/L/h). D-allose is a rare sugar used as a non-caloric and non-toxic sweetener [8]; it has attracted increasing research interest owing to its beneficial medical properties, including anti-cancer, anti-oxidant, anti-inflammatory, and anti-hypertensive effects [11]. Moreover, SmGI can isomerize D-glucose, D-xylose, D-ribose, and L-rhamnose to D-fructose, D-xylulose, D-ribulose, and L-rhamnulose, respectively [11]. Thus, besides their normal ability to interconvert D-glucose/D-fructose and D-xylose/D-xylulose, GIs can also produce rare sugars that are used in food or medicinal products. GIs from various species could be developed for industrial applications by exploiting their intrinsic substrate specificity for the isomerization for rare sugars.

2.2. Metal Ions

GI requires divalent cations as cofactors for its isomerization activity [12]. Typically, GI is known to exhibit the highest activity in the presence of divalent metal ions such as Mg^{2+}, Mn^{2+} and Co^{2+}; however, the specific metal ion requirement can vary depending on the source of the enzyme. For example, the GI from *Bacillus coagulans* shows the maximum enzyme activity in the presence of Mg^{2+} or Mn^{2+} [13], and Mn^{2+} is the most favorable ion for catalytic activity of the GI from *Piromyces* sp. E2 [14]; in contrast, the GI from the *Streptomyces* strain YT-5 prefers Co^{2+} [15]. Moreover, using a combination of these divalent metal ions has been shown to further enhance the isomerization activity. For example, the activity of EDTA-treated GI from *Streptomyces* sp. CH7 was reportedly increased by 3.6-, 2.8-, and 2.1-fold in the presence of 1 mM Mg^{2+}, Mn^{2+}, and Co^{2+}, respectively, compared to its activity in the absence of any metal ions [16]. However, the enzyme activity increased 6.2-fold and 44.2-fold in the presence of the combinations 1 mM Mg^{2+} and 0.1 mM Co^{2+}, and 10 mM Mg^{2+} and 0.1 mM Co^{2+}, respectively [16]. Thus, during optimization, it is important to measure GI activity not only with one metal ion, but also with a combination of several metal ions. In general, Mg^{2+} and Mn^{2+} act as GI activators, whereas Co^{2+} acts as a protein stabilizer, maintaining the ordered conformation in the quaternary structure of GI [1].

2.3. Reaction Mechanism

The catalytic reaction of GI occurs in three major steps: (i) ring opening, (ii) isomerization, and (iii) ring closure [17] (Figure 2). The action of GI has been attributed to a hydride shift mechanism, based on results from several studies employing chemical modification, X-ray crystallography, and isotope exchange methods [18–20]. Accordingly, it is proposed that the substrate at the active site of GI exists in an open ring state, and a closed ring form product is created after isomerization via a hydride shift from C2 to C1 [18–20]. During this process, a conserved histidine residue catalyzes the proton transfer from O1 to O5. Crystallographic studies have shown that, during its isomerization, xylose initially binds to the enzyme in an open chain conformation. The GI structure contains two sites (M1 and M2) for metal binding. The metal ion at the M1 site binds to O2 and O4 of the xylose molecule, and once bound, the metal ion at the M2 site binds to O1 and O2 in the transition

state. These interactions, along with a conserved lysine residue, help catalyze the hydride shift necessary for isomerization [18–20].

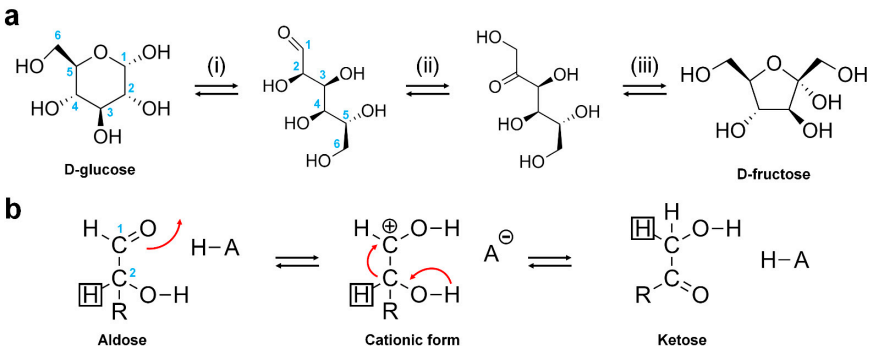

Figure 2. Isomerization mechanism of GI. (**a**) Three major steps involved in the configuration change from D-glucose to D-fructose catalyzed by GI. (**b**) Hydride shift mechanism of GI.

3. Structure

3.1. Overall Structure

The first crystal structure of GI was reported from *Streptomyces rubiginosus* at a 4 Å resolution in 2001 [21]. To date, more than 120 crystal structures of GI/XIs from various species, such as *S. rubiginosus*, *Arthrobacter* sp. NRRL B3728, *Piromyces* sp. E2, *Actinoplanes missouriensis*, *Streptomyces olivochromogenes*, *Streptomyces diastaticus*, *Streptomyces* sp. F-1, *Streptomyces* sp. SK, *Bacteroides thetaiotaomicron* VPI-5482, *Geobacillus stearothermophilus*, *Paenibacillus* sp. R4, *Streptomyces albus*, *S. murinus*, *Thermoanaerobacterium thermosulfurigenes*, *Thermotoga neapolitana*, *Thermus caldophilus*, and *Thermus thermophilus* HB8, have been elucidated and deposited in the Protein Data Bank (PDB, www.rcsb.org). These include more than 100 crystal structures of the GI from *S. rubiginosus*; however, many of these structures have been solved and used only as model samples for the development of various X-ray technologies or studying radiation damage, because the GI from *S. rubiginosus* exhibits high-quality diffraction intensity [22–29].

Structurally, GI consists of a TIM barrel-like domain and an extended α-helix domain (Figure 3A,B) which are assembled into a functional tetramer (Figure 3C) [21]. The substrate-binding pocket is formed by two protomers and the GI active site is located on the TIM-barrel fold (Figure 3C). The GI exists as a tetramer with 222 crystallographic symmetry [30] and includes four active sites for substrate isomerization.

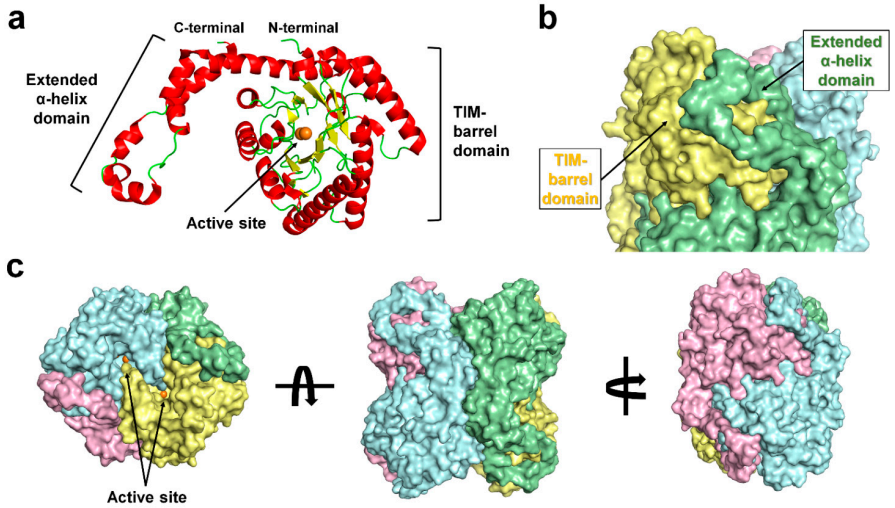

Figure 3. Crystal structure of the GI from *Streptomyces rubiginosus* (SruGI). (**a**) GI protomer consists of a TIM-barrel domain and an extended α-helical domain. (**b**) The extended α-helical domain interacts with the TIM barrel domain from neighboring GI molecule. (**c**) Tetrameric GI shows 222 symmetry.

The typical GI active site contains two sites, M1 and M2, for metal binding. M1 and M2 are referred to as the structural metal and catalytic metal sites, respectively [31], as the metals bound at the M1 and M2 sites are involved in the substrate binding and isomerization mechanism, respectively. In *S. rubiginosus*, the metal at the M1 site is coordinated by Glu181, Glu217, Asp245, and Asp287, and the metal at the M2 site binds the protein via Glu217, His220, Asp255, and Asp257. These metal-bound amino acids are conserved across the GI family [32,33] (Figure 4).

Most of the crystal structures of GI are bound to the metal ions Mg^{2+}, Mn^{2+}, or Co^{2+}, which are involved in the isomerase activity [1]. However, some GI crystal structures are known to contain biologically less related metal ions in their active sites [34,35]. For example, in the crystal structures of GIs from *S. rubiginosus* (PDB code: 4W4Q) [36], *Paenibacillus* sp. *R4* (PDB code: 6INT) [34], and *Piromyces* (6T8E) [35], Ca^{2+} is located in the M1 and M2 sites of the active site, although enzyme activity in the presence of Ca^{2+} has not been verified. In addition, in some crystal structures, the metal ion was placed in a position other than at the M1 and M2 sites [37]. Thus, metal ions in the crystal structures of GI require verification through biochemical experiments or X-ray analysis; additionally, precise analysis of electron density is required to confirm their position and involvement in GI substrate binding and activity.

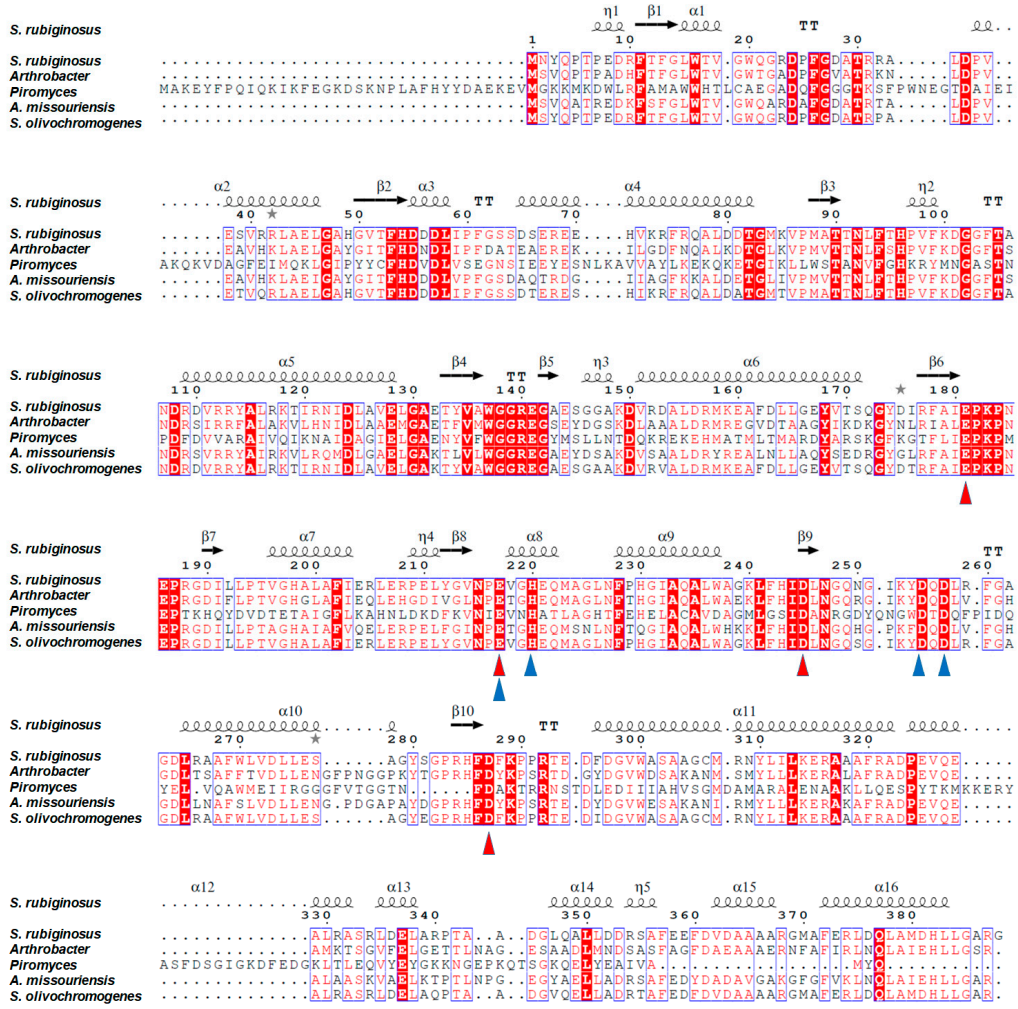

Figure 4. Amino acid sequence alignment of GIs from *Streptomyces rubiginosus* (UniProt Accession: P24300), *Arthrobacter* sp. NRRL B3728 (P12070), *Piromyces* sp. E2 (Q9P8C9), *Actinoplanes missouriensis* (P12851), and *Streptomyces olivochromogenes* (P15587). Residues involved in metal binding at the M1 and M2 sites are indicated by red and blue triangles, respectively. Alignment was performed using Clustal Omega [38] and displayed using Espript [39].

3.2. Metal-Binding State at the GI Active Site

With regard to metal binding, the active site of GI can exist in three different states: (i) two-metal-binding state, (ii) one-metal-binding state, and (iii) metal free-state (Figure 5) [23,33,40]. Although GI crystal structures exhibit different metal-binding states at their active site, the overall GI fold is almost similar, indicating that metal binding does not influence the overall protein folding [40].

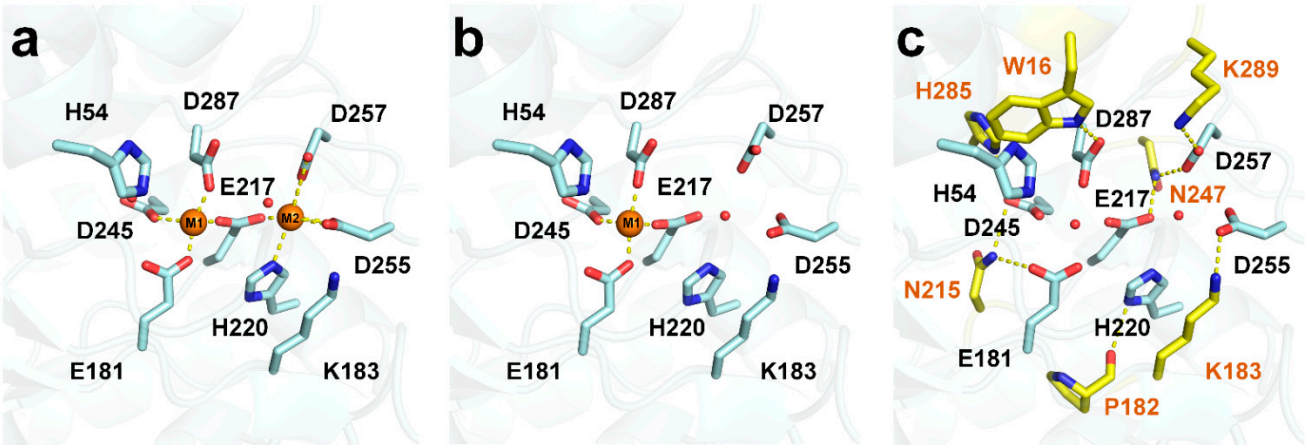

Figure 5. Three different metal-binding states in the active site of the GI from *Streptomyces rubiginosus* (SruGI). (**a**) Two-metal-binding mode (PDB code: 6IRK), (**b**) one-metal-binding mode (PDB code: 5Y4I), and (**c**) metal-free state of SruGI (PDB code: 7CJP).

In the two-metal- binding state of GI, the M1 and M2 sites at active site are occupied by divalent metal ions such as Mg^{2+}, Mn^{2+}, and Co^{2+}, and the differences in enzyme activity occur depending on the metal occupying the active site [41,42]. In the crystal structure of the GI from *S. rubiginosus*, determined via cryo-crystallography, the metal ion at the M1 site is coordinated by Glu181, Glu217, Asp245, and Asp287, as well as the glycerol or ethylene glycol molecule, which is used as a cryoprotectant [33,40]. Meanwhile, in the room-temperature structure of *S. rubiginosus* GI, the metal ion at the M1 site is coordinated by the conserved metal-binding residues and water molecules [23,37], and the metal ion at the M2 site is coordinated by the conserved Glu217, His220, Asp255 (binate interaction), Asp257, and water molecules. The distance between the metal-binding residues and the metal is shorter at the M1 site than at the M2 site, indicating that the M1 site has tighter metal–protein interactions than the M2 site.

In the one-metal-binding mode of GI, the metal ion exists only at the M1 site involved in substrate recognition [33], indicating the higher affinity of the M1 site for metal binding than the M2 site. This result is consistent with the tighter interaction previously observed between the metal-binding residues and the metal at the M1 site, than the interaction at the M2 site [37]. In the one-metal-binding mode, the sugar substrate or inhibitor can interact with the metal ion at the M1 site [33]. However, isomerization activity through a hydride shift mechanism cannot occur due to the absence of a metal ion at the M2 site, leading to an inactive state of GI.

In the metal-free state of GI, no metal is found at both the M1 and M2 sites [40]. In this state, the substrate cannot bind to the active site because neither the metal binding to the M2 site involved in the isomerization activity nor the metal of the M1 site to which the substrate binds exist. In the metal-free state, conformation changes in conserved metal-binding residues occur within 1 Å despite the absence of metal ions at the two metal sites [40]. This is attributed to stabilization of the position of the metal-binding residues by the neighboring residues around the active sites (Glu181 *-Asn215, Glu217 *-Asn247, His220 *-Pro182, Asp245 *-Asn215, Asp245 *-His285, Asp255 *-Lys183, Asp257 *-Asn247, Asp257 *-Lys289, and Asp287 *-Trp16; metal-binding residues are indicated by an asterisk),

which helps them maintain their positions without large conformational changes [40]. Accordingly, the metal-free state exhibits a minimum open configuration for the metal to perceive and bind to the sites [40]. Based on the existing biochemical knowledge, this study proposed that, when combining with GI in a metal-free state, the metal first binds to the M1 site and then is filled in the M2 site.

3.3. Xylitol Binding to the Active Site of GI

Structure-based inhibitor studies of GI are helpful for industrial applications such as HGFS and bioethanol production [37], by identifying the parameters of enzyme engineering to prevent product inhibition. The isomerase activity of GI can be inhibited by some divalent cations such as Ca^{2+}, Cu^{2+}, Zn^{2+}, Ni^{2+}, Ag^{2+}, and Hg^{2+} [1]. In addition, molecules such as xylitol, arabitol, sorbitol, mannitol, lyxose, and Tris also inhibit GI activity [43]. However, the mechanism of GI inhibition by these compounds remains largely unclear.

Among these compounds, the inhibition of the activity of GI by xylitol, which is a structural analogue of xylose, has been well studied [44,45]. To date, six crystal structures of xylitol-bound GI have been deposited in PDB (PDB code 1XIG, 2XIS, 3GNX, 4DUO, 5Y4J, and 7DFK) [31,33,37,46,47]. All these structures reveal that the xylitol molecule binds at the M1 site in the active site of GI. Three oxygen (O2, O3, and O4) atoms from xylitol interact with the metal ion at the M1 site, and the metal ion is stabilized by octahedral coordination, by the metal-interacting residues of the enzyme, and the xylitol molecules [31,33,37,46,47]. Therefore, xylitol binding in the M1 site prevents substrate access to the metal ion. The crystal structure of one-metal-binding mode of GI shows that the metal ion at the M2 site is not essential to facilitate xylitol binding to the M1 site [33]. Furthermore, xylitol binding to the M1 site stabilizes the geometry of the metal-binding sites.

Meanwhile, the xylitol-bound GI structure shows a high B-factor value of the metal ion at the M2 site, although the reason for this observation remains unknown. A recently obtained room-temperature structure of xylitol-bound GI via serial crystallography revealed a correlation between xylitol binding and low metal occupancy at the M2 site [37]. In native GI, the M1 site shows a distorted octahedral coordination, but it is geometrically stabilized upon xylitol binding to the metal at the M1 site [37] (Figure 6A). This causes a rearrangement of the conformation of metal-binding residues in the M2 site (Figure 6C). This induces the distortion of metal coordination at the M2 site, leading to the release of the unstable coordinated metal ion from the M2 site [37]. This metal release induces further conformational changes in the neighboring residues (Figure 6C). Since the metal ion at the M2 site involved in isomerization activity is released as a result of xylitol binding, an additional catalytic metal ion has to be added for an isomerization reaction in industrial applications after the release of xylitol.

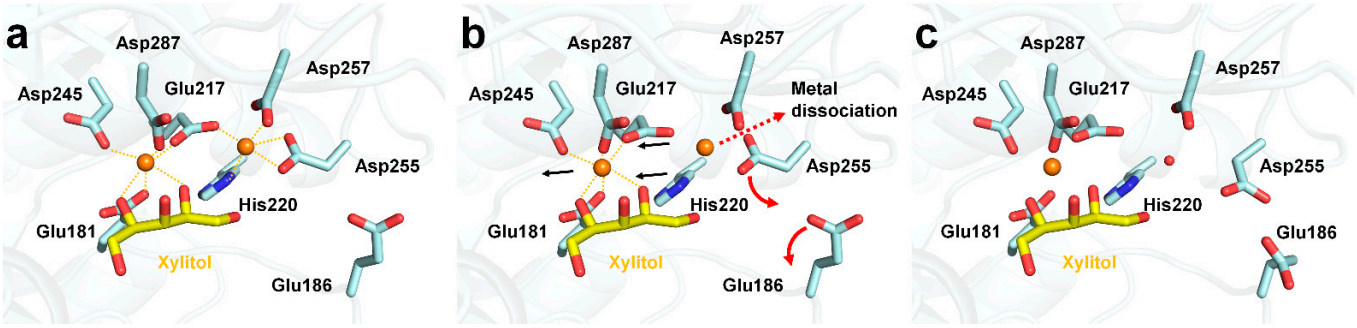

Figure 6. Proposed mechanism of xylitol-induced release of metal at the M2 site of GI. (**a**) Xylitol-bound state of GI. (**b**) Rearrangement of xylitol-binding residues. (**c**) Release of metal ion from M2 site of GI.

4. Application of GI

4.1. High-Fructose Corn Syrup (HFCS)

Owing to its beneficial properties, including a high solubility at low temperature, a lower tendency to crystallize than sucrose, and a high freezing point depression, fructose is widely used in the manufacture of ice cream and frozen desserts to influence taste and texture [48]. Fructose is also used in the production of cake, biscuits, bread, and other confectionery products [49,50]. Moreover, fructose increases the shelf-life of food products, with its high osmotic pressure in solution, making it a better preservative against microbial growth than sucrose syrup [51]. Additionally, fructose is used in the pharmaceutical industry to manufacture diabetes medicine, as it does not influence the blood levels of glucose and insulin [52].

HFCS is an equilibrium mixture of glucose and fructose, which has the advantages of sweetness, low cost, and high solubility [53]. Depending on the fructose content, HFCS can be classified as HFCS-42 (42% fructose, 53% glucose, and 5% polysaccharide), HFCS-55 (55% fructose, 42% glucose, and 3% polysaccharide), and HFCS-90 (90% fructose, 9% glucose and 1% polysaccharide) [54]. Among them, HFCS-55 is the most commonly used, with its commercial production involving several processes such as chromatography, purification, and concentration [55].

HFCS is widely applied in the food, detergent, and pharmaceutical industries [56]. Although glucose can be converted to fructose using a chemical process for HFCS production, this chemical reaction is non-specific and leads to the formation of non-metabolizable sugars [4]. In contrast, GI catalyzes the isomerization of glucose to fructose with excellent specificity, which is critical for the industrial production and application of HFCS [4].

As GI exhibits a reversible isomerization activity, a thermodynamic equilibrium exists in the isomerization reaction between glucose and fructose [57]. The rate of the enzymatic conversion of glucose to fructose can be increased by increasing the reaction temperature; therefore, using a highly thermostable GI capable of sustained operation at high temperatures is critical for one-step HFCS production [57].

Brown et al. reported a GI from the thermophilic eubacterium *Thermotoga maritima* (TmaGI) [58], which is produced when the bacterium is grown in the presence of xylose. TmaGI requires the metal cations Co^{2+} and Mg^{2+} for enzyme activity [58]. This enzyme prefers xylose as a substrate and is most active at pH 6.5–7.5. TmaGI displays the maximum activity at an optimum temperature of 105 to 110 °C, and its half-life is approximately 10 min at 120 °C and pH 7.0. TmaGI is a promising candidate for improving the efficiency of the industrial glucose isomerization process, as it exhibits optimal pH from neutral to slightly acidic, as well as a high thermostability [58].

Deng et al. reported the characterization of GI from *Thermobifida fusca* WSH03-11 (TfuGI) [59]. TfuGI displayed the maximum activity at an optimum temperature of 80 °C, with a half-life of approximately 2 h at 80 °C or 15 h at 70 °C. TfuGI was the most active at pH 10 and retained 95% of its initial activity after incubation at pH 5–10 and 4 °C for 24 h. Analysis of TfuGI enzyme kinetics revealed the K_m and k_{cat} values to be 197 mM and 1688 min^{-1}, respectively [59]. TfuGI was able to convert glucose (45% *w*/*v*) to fructose, with a maximum conversion yield of 53% at pH 7.5 and 70 °C.

Jia et al. have characterized GIs from *Thermoanaerobacterium xylanolyticum* (TxyGI), *Thermus oshimai* (TosGI), *Geobacillus thermocatenulatus* (GthGI), and *Thermoanaerobacter siderophilus* (TsiGI) [60]. These enzymes were identified using a genome mining approach for their potential application in manufacturing HFCS at elevated temperatures with a low cost of enriching syrups. Among these enzymes, TosGI showed the highest catalytic efficiency toward D-glucose, along with superior thermostability. The optimum temperature of TosGI was 95 °C, and it retained more than 80% of its activity after 48 h at 85 °C in the presence of 20 mM Mn^{2+} [60]. The kinetic parameters K_m and k_{cat}/K_m of TosGI were calculated to be 81.46 mM and 21.77 min^{-1} mM^{-1}, respectively [60]. TosGI achieved a maximum yield of 52.16% for the conversion of D-glucose (400 g/L) to D-fructose at 85 °C [60].

The GI from *Caldicellulosiruptor bescii* (CbeGI), characterized by Dai et al. [57], exhibited the maximum activity at pH 7.0 and 80 °C and retained good thermostability at 85 °C. CbeGI showed affinity for D-glucose, with a K_m of 42.61 mM, and a conversion efficiency up to 57.3% with 3 M D-glucose [57]. The high catalytic efficiency and affinity of CbeGI make it a valuable enzyme for the direct production of 55% HFCS.

Vieille et al. reported the characterization of GI from the hyperthermophile *T. neapolitana* 5068 (TnGI) [61]. The optimal temperature of TnGI was above 95 °C and the optimum pH was 7.1, but the enzyme also showed high activity over a wide pH range. Kinetics studies showed that the catalytic efficiency (k_{cat}/K_m) of TnGI remained constant between 60 and 90 °C; however, the catalytic efficiency decreased between 90 and 98 °C, primarily because of a large increase in K_m [61]. TnGI had a higher turnover number and a lower Km for glucose compared to other thermophilic GIs [61]. Taken together, thermophilic GIs exhibit various activities according to the species of origin and are expected to be extensively applied in industrial HFCS production.

4.2. Ethanol Production

The bioconversion of a renewable biomass into ethanol is attractive in view of the rapid depletion of fossil fuels [62]. GI can catalyze the isomerization of xylose derived from hemicellulosic biomass to xylulose, which can be fermented to ethanol by conventional yeast such as *Saccharomyces cerevisiae*, *Schizosaccharomyces pombe*, and *Candida tropicalis* [63–65]. This property of GI is attractive for the application in bioethanol production because no coenzyme is required and no intermediates are produced during the reaction [66]. However, the typical ethanol production process is plagued by low efficiency, owing to the low conversion yield of xylose to ethanol [67]. The GI enzyme engineering and strain improvement approaches have been explored to improve the conversion yield of xylose to ethanol [1,65,68]. The engineering of yeast strains that exhibit faster xylose metabolism is important in pursuing strain improvement for bioethanol production [69,70].

Ko et al. evaluated the performance of SXA-R2P-E, an engineered isomerase-based xylose-utilizing *S. cerevisiae* strain, for co-fermentation of xylose and glucose to ethanol [65]. SXA-R2P-E produced 50g/L ethanol (yield of 0.43 g ethanol/g sugar) in 72 h via a high-sugar fermentation process (70 g/L glucose and 40 g/L xylose). This strain also produced 18-21 g/L ethanol (yield of 0.43–0.46 g ethanol/g sugar) from acid-pretreated lignocellulosic hydrolysates such as rice straw and hardwood [65].

Seike et al. reported improved xylose fermentation through XI expression in the xylose-utilizing *S. cerevisiae* strain IR-2, which has a deletion of the *GR3* gene (encoding an endogenous xylose reductase) and overexpresses *XK21* (encoding an additional xylulose kinase). Evolutionary engineering was performed in the IR-2 strain to select high-efficiency XIs from eight previously reported XIs derived from various species [68]: *Burkholderia cenocepacia* J2315 [71], *Lachnoclostridium phytofermentans ISDg* (LpXI) [67], *Orpinomyces* sp. ukk1 [72], *Piromyces* sp. E2 [73], *Prevotella ruminicola* TC2-24 [74], *Ruminiclostridium cellulolyticum* H10 [75], *Ruminococcus flavefaciens* 17 [76], and *S. rubiginosus* [77]. Among them, the strain expressing LpXI exhibited the highest D-xylose consumption rate after 72 h of micro-aerobic fermentation on D-glucose and D-xylose mixed medium [68]. Furthermore, to enhance the LpXI catalytic activity, the authors performed random mutagenesis using an error-prone polymerase chain reaction and obtained two enzyme constructs with improved fermentation performances [68]. The SS120 strain, expressing double mutant LpXI (T63I/V162A), produced 53.3 g/L ethanol in 72 h (ethanol yield of approximately 0.44 (g/g-input sugars) from 85 g/L D-glucose and 35 g/L D-xylose [68].

XI enzyme engineering is another approach that has been employed to increase the efficiency of bioethanol production by accelerating xylose metabolism [68,78]. For example, the XI from the fungal strain *Piromyces* sp. E2 (PirXI) is employed for xylose isomerization in engineered *S. cerevisiae* strains but has low activity in vivo. To improve the performance of PirXI, Lee et al. constructed a mutant library by substituting residues around the substrate and metal-binding sites of the enzyme [35]. PirXI variants were obtained by transferring

the library to *S. cerevisiae*, followed by in vivo selection for enhanced xylose-supported growth under aerobic and anaerobic conditions. In particular, in the presence of Mg^{2+} or Mn^{2+}, the K_m of PirXI-V270A/A273G variant for xylose was higher, and the k_{cat} was lower than the corresponding values for wild-type PirXI [35].

Thus, further efforts to engineer GI/XI for a high xylose conversion rate through rational engineering or directed evolution are still needed, and applied research should be performed through in vivo studies on improved strains to enable efficient bioethanol production.

5. Perspective

In addition to its biological importance, GI is an industrially important enzyme that is applied in HFCS and bioethanol production. Although biochemical and structural studies have been conducted on GIs from various organisms, many GIs still need to be identified from the protein database. The development of more efficient GI-based industrial processes requires extensive biochemical analysis and engineering of novel GIs. In addition, it will be necessary to analyze not only in vitro enzymatic activity, but also the industrial performance of GI using whole cell systems. On the other hand, structural studies on the inhibition of GI activity by various metals, sugars, and other inhibitors should be conducted to help better modulate GI activity and enhance the enzyme performance during industrial application. Furthermore, it is necessary to understand the dynamical structural changes occurring in GI to aid enzyme engineering efforts, as most GI structures currently collected in cryogenic environments have only provided limited knowledge with regard to flexibility. The recently developed serial crystallography technique provides information regarding the molecular fluidity of proteins at room temperature, and future studies of molecular fluidity based on the room-temperature crystal structures will provide useful information for GI enzyme engineering.

Funding: This work was funded by the National Research Foundation of Korea (NRF) (NRF-2017R1D1A1B03033087, NRF-2017M3A9F6029736 and NRF-2021R1I1A1A01050838) and Korea Initiative for Fostering University of Research and Innovation (KIURI) Program of the NRF (NRF-2020M3H1A1075314).

Institutional Review Board Statement: Not applicable.

Informed Consent Statement: Not applicable.

Data Availability Statement: The data presented in this study are available on request from the corresponding author. The data are not publicly available due to data protection legislation.

Conflicts of Interest: The author declares no conflict of interest.

References

1. Bhosale, S.H.; Rao, M.B.; Deshpande, V.V. Molecular and industrial aspects of glucose isomerase. *Microbiol. Rev.* **1996**, *60*, 280–300. [CrossRef]
2. Kilara, A.; Shahani, K.M. The use of immobilized enzymes in the food industry: A review. *CRC Crit. Rev. Food Sci. Nutr.* **1979**, *12*, 161–198. [CrossRef]
3. Deshpande, V.; Rao, M. Glucose Isomerase. In *Enzyme Technology*; Springer: New York, NY, USA, 2006; pp. 239–252. [CrossRef]
4. Singh, R.S.; Singh, T.; Pandey, A. Microbial Enzymes—An Overview. In *Advances in Enzyme Technology*; Elsevier: Amsterdam, The Netherlands, 2019; pp. 1–40. [CrossRef]
5. Kasumi, T.; Hayashi, K.; Tsumura, N. Purification and Enzymatic Properties of Glucose Isomerase from *Streptomyces griseofuscus*, S-41. *Agric. Biol. Chem.* **2014**, *45*, 619–627. [CrossRef]
6. Kim, Y.-S.; Kim, D.-Y.; Park, C.-S. Production of l-rhamnulose, a rare sugar, from l-rhamnose using commercial immobilized glucose isomerase. *Biocatal. Biotransform.* **2017**, *36*, 417–421. [CrossRef]
7. Langan, P.; Sangha, A.K.; Wymore, T.; Parks, J.M.; Yang, Z.K.; Hanson, B.L.; Fisher, Z.; Mason, S.A.; Blakeley, M.P.; Forsyth, V.T.; et al. L-Arabinose binding, isomerization, and epimerization by D-xylose isomerase: X-ray/neutron crystallographic and molecular simulation study. *Structure* **2014**, *22*, 1287–1300. [CrossRef] [PubMed]
8. Chen, Z.; Chen, J.; Zhang, W.; Zhang, T.; Guang, C.; Mu, W. Recent research on the physiological functions, applications, and biotechnological production of D-allose. *Appl. Microbiol. Biotechnol.* **2018**, *102*, 4269–4278. [CrossRef] [PubMed]
9. Fehér, C. Novel approaches for biotechnological production and application of L-arabinose. *J. Carbohydr. Chem.* **2018**, *37*, 251–284. [CrossRef]

10. Menavuvu, B.T.; Poonperm, W.; Leang, K.; Noguchi, N.; Okada, H.; Morimoto, K.; Granstrom, T.B.; Takada, G.; Izumori, K. Efficient biosynthesis of D-allose from D-psicose by cross-linked recombinant L-rhamnose isomerase: Separation of product by ethanol crystallization. *J. Biosci. Bioeng.* **2006**, *101*, 340–345. [CrossRef] [PubMed]
11. Choi, M.N.; Shin, K.C.; Kim, D.W.; Kim, B.J.; Park, C.S.; Yeom, S.J.; Kim, Y.S. Production of D-Allose From D-Allulose Using Commercial Immobilized Glucose Isomerase. *Front. Bioeng. Biotechnol.* **2021**, *9*, 681253. [CrossRef]
12. Young, J.M.; Schray, K.J.; Mildvan, A.S. Proton magnetic relaxation studies of the interaction of D-xylose and xylitol with D-xylose isomerase. Characterization of metal-enzyme-substrate interactions. *J. Biol. Chem.* **1975**, *250*, 9021–9027. [CrossRef]
13. Yoshimura, S.; Danno, G.-i.; Natake, M. Studies ond-Glucose Isomerizing Activity ofd-Xylose Grown Cells from *Bacillus coagulans*, Strain HN-68. *Agric. Biol. Chem.* **2014**, *30*, 1015–1023. [CrossRef]
14. Lee, M.; Rozeboom, H.J.; de Waal, P.P.; de Jong, R.M.; Dudek, H.M.; Janssen, D.B. Metal Dependence of the Xylose Isomerase from *Piromyces* sp. E2 Explored by Activity Profiling and Protein Crystallography. *Biochemistry* **2017**, *56*, 5991–6005. [CrossRef] [PubMed]
15. Takasaki, Y. Studies on Sugar-isomerizing Enzyme. *Agric. Biol. Chem.* **2014**, *30*, 1247–1253. [CrossRef]
16. Chanitnun, K.; Pinphanichakarn, P. Glucose(xylose) isomerase production by Streptomyces sp. CH7 grown on agricultural residues. *Braz. J. Microbiol.* **2012**, *43*, 1084–1093. [CrossRef] [PubMed]
17. Kovalevsky, A.Y.; Hanson, L.; Fisher, S.Z.; Mustyakimov, M.; Mason, S.A.; Forsyth, V.T.; Blakeley, M.P.; Keen, D.A.; Wagner, T.; Carrell, H.L.; et al. Metal ion roles and the movement of hydrogen during reaction catalyzed by D-xylose isomerase: A joint x-ray and neutron diffraction study. *Structure* **2010**, *18*, 688–699. [CrossRef] [PubMed]
18. Lee, C.Y.; Bagdasarian, M.; Meng, M.H.; Zeikus, J.G. Catalytic mechanism of xylose (glucose) isomerase from Clostridium thermosulfurogenes. Characterization of the structural gene and function of active site histidine. *J. Biol. Chem.* **1990**, *265*, 19082–19090. [CrossRef]
19. Collyer, C.A.; Henrick, K.; Blow, D.M. Mechanism for aldose-ketose interconversion by D-xylose isomerase involving ring opening followed by a 1,2-hydride shift. *J. Mol. Biol.* **1990**, *212*, 211–235. [CrossRef]
20. Collyer, C.A.; Blow, D.M. Observations of reaction intermediates and the mechanism of aldose-ketose interconversion by D-xylose isomerase. *Proc. Natl. Acad. Sci. USA* **1990**, *87*, 1362–1366. [CrossRef]
21. Carrell, H.L.; Rubin, B.H.; Hurley, T.J.; Glusker, J.P. X-ray crystal structure of D-xylose isomerase at 4 Å resolution. *J. Biol. Chem.* **1984**, *259*, 3230–3236. [CrossRef]
22. Taberman, H.; Bury, C.S.; van der Woerd, M.J.; Snell, E.H.; Garman, E.F. Structural knowledge or X-ray damage? A case study on xylose isomerase illustrating both. *J. Synchrotron Radiat.* **2019**, *26*, 931–944. [CrossRef]
23. Lee, D.; Baek, S.; Park, J.; Lee, K.; Kim, J.; Lee, S.J.; Chung, W.K.; Lee, J.L.; Cho, Y.; Nam, K.H. Nylon mesh-based sample holder for fixed-target serial femtosecond crystallography. *Sci. Rep.* **2019**, *9*, 6971. [CrossRef] [PubMed]
24. Lee, K.; Lee, D.; Baek, S.; Park, J.; Lee, S.J.; Park, S.; Chung, W.K.; Lee, J.L.; Cho, H.S.; Cho, Y.; et al. Viscous-medium-based crystal support in a sample holder for fixed-target serial femtosecond crystallography. *J. Appl. Crystallogr.* **2020**, *53*, 1051–1059. [CrossRef]
25. Nam, K.H. Stable sample delivery in viscous media via a capillary for serial crystallography. *J. Appl. Crystallogr.* **2020**, *53*, 45–50. [CrossRef]
26. Nam, K.H. Shortening injection matrix for serial crystallography. *Sci. Rep.* **2020**, *10*, 107. [CrossRef] [PubMed]
27. Nam, K.H. Polysaccharide-Based Injection Matrix for Serial Crystallography. *Int. J. Mol. Sci.* **2020**, *21*, 3332. [CrossRef] [PubMed]
28. Nam, K.H. Lard Injection Matrix for Serial Crystallography. *Int. J. Mol. Sci.* **2020**, *21*, 5977. [CrossRef] [PubMed]
29. Park, S.Y.; Choi, H.; Eo, C.; Cho, Y.; Nam, K.H. Fixed-Target Serial Synchrotron Crystallography Using Nylon Mesh and Enclosed Film-Based Sample Holder. *Crystals* **2020**, *10*, 803. [CrossRef]
30. Dauter, Z.; Dauter, M.; Hemker, J.; Witzel, H.; Wilson, K.S. Crystallisation and preliminary analysis of glucose isomerase from *Streptomyces albus*. *FEBS Lett.* **1989**, *247*, 1–8. [CrossRef]
31. Whitlow, M.; Howard, A.J.; Finzel, B.C.; Poulos, T.L.; Winborne, E.; Gilliland, G.L. A metal-mediated hydride shift mechanism for xylose isomerase based on the 1.6 Å *Streptomyces rubiginosus* structures with xylitol and D-xylose. *Proteins* **1991**, *9*, 153–173. [CrossRef]
32. Carrell, H.L.; Glusker, J.P.; Burger, V.; Manfre, F.; Tritsch, D.; Biellmann, J.F. X-ray analysis of D-xylose isomerase at 1.9 A: Native enzyme in complex with substrate and with a mechanism-designed inactivator. *Proc. Natl. Acad. Sci. USA* **1989**, *86*, 4440–4444. [CrossRef]
33. Bae, J.E.; Kim, I.J.; Nam, K.H. Crystal structure of glucose isomerase in complex with xylitol inhibitor in one metal binding mode. *Biochem. Biophys. Res. Commun.* **2017**, *493*, 666–670. [CrossRef]
34. Park, S.H.; Kwon, S.; Lee, C.W.; Kim, C.M.; Jeong, C.S.; Kim, K.J.; Hong, J.W.; Kim, H.J.; Park, H.H.; Lee, J.H. Crystal Structure and Functional Characterization of a Xylose Isomerase (PbXI) from the Psychrophilic Soil Microorganism, *Paenibacillus* sp. *J. Microbiol. Biotechnol.* **2019**, *29*, 244–255. [CrossRef]
35. Lee, M.; Rozeboom, H.J.; Keuning, E.; de Waal, P.; Janssen, D.B. Structure-based directed evolution improves *S. cerevisiae* growth on xylose by influencing in vivo enzyme performance. *Biotechnol. Biofuels* **2020**, *13*, 5. [CrossRef]
36. Sugahara, M.; Mizohata, E.; Nango, E.; Suzuki, M.; Tanaka, T.; Masuda, T.; Tanaka, R.; Shimamura, T.; Tanaka, Y.; Suno, C.; et al. Grease matrix as a versatile carrier of proteins for serial crystallography. *Nat. Methods* **2015**, *12*, 61–63. [CrossRef]
37. Nam, K.H. Room-Temperature Structure of Xylitol-Bound Glucose Isomerase by Serial Crystallography: Xylitol Binding in the M1 Site Induces Release of Metal Bound in the M2 Site. *Int. J. Mol. Sci.* **2021**, *22*, 3892. [CrossRef]

38. Sievers, F.; Wilm, A.; Dineen, D.; Gibson, T.J.; Karplus, K.; Li, W.; Lopez, R.; McWilliam, H.; Remmert, M.; Soding, J.; et al. Fast, scalable generation of high-quality protein multiple sequence alignments using Clustal Omega. *Mol. Syst. Biol.* **2011**, *7*, 539. [CrossRef]
39. Gouet, P.; Courcelle, E.; Stuart, D.I.; Metoz, F. ESPript: Analysis of multiple sequence alignments in PostScript. *Bioinformatics* **1999**, *15*, 305–308. [CrossRef]
40. Nam, K.H. Crystal structure of the metal-free state of glucose isomerase reveals its minimal open configuration for metal binding. *Biochem. Biophys. Res. Commun.* **2021**, *547*, 69–74. [CrossRef] [PubMed]
41. Sudfeldt, C.; Schaffer, A.; Kagi, J.H.; Bogumil, R.; Schulz, H.P.; Wulff, S.; Witzel, H. Spectroscopic studies on the metal-ion-binding sites of Co^{2+}-substituted D-xylose isomerase from *Streptomyces rubiginosus*. *Eur. J. Biochem.* **1990**, *193*, 863–871. [CrossRef] [PubMed]
42. Callens, M.; Kerstershilderson, H.; Vangrysperre, W.; Debruyne, C.K. D-Xylose Isomerase from *Streptomyces violaceoruber:* Structural and Catalytic Roles of Bivalent-Metal Ions. *Enzym. Microb. Technol.* **1988**, *10*, 695–700. [CrossRef]
43. Smith, C.A.; Rangarajan, M.; Hartley, B.S. D-Xylose (D-glucose) isomerase from *Arthrobacter* strain N.R.R.L. B3728. Purification and properties. *Biochem. J.* **1991**, *277*, 255–261. [CrossRef] [PubMed]
44. Fenn, T.D.; Ringe, D.; Petsko, G.A. Xylose isomerase in substrate and inhibitor michaelis states: Atomic resolution studies of a metal-mediated hydride shift. *Biochemistry* **2004**, *43*, 6464–6474. [CrossRef] [PubMed]
45. Volkin, D.B.; Klibanov, A.M. Mechanism of thermoinactivation of immobilized glucose isomerase. *Biotechnol. Bioeng.* **1989**, *33*, 1104–1111. [CrossRef]
46. Carrell, H.L.; Hoier, H.; Glusker, J.P. Modes of binding substrates and their analogues to the enzyme D-xylose isomerase. *Acta Crystallogr. D Biol. Crystallogr.* **1994**, *50*, 113–123. [CrossRef]
47. Kovalevsky, A.; Hanson, B.L.; Mason, S.A.; Forsyth, V.T.; Fisher, Z.; Mustyakimov, M.; Blakeley, M.P.; Keen, D.A.; Langan, P. Inhibition of D-xylose isomerase by polyols: Atomic details by joint X-ray/neutron crystallography. *Acta Crystallogr. D Biol. Crystallogr.* **2012**, *68*, 1201–1206. [CrossRef]
48. White, J.S. Straight talk about high-fructose corn syrup: What it is and what it ain't. *Am. J. Clin. Nutr.* **2008**, *88*, 1716S–1721S. [CrossRef]
49. Sahin, A.W.; Zannini, E.; Coffey, A.; Arendt, E.K. Sugar reduction in bakery products: Current strategies and sourdough technology as a potential novel approach. *Food Res. Int.* **2019**, *126*, 108583. [CrossRef]
50. Zargaraan, A.; Kamaliroosta, L.; Yaghoubi, A.S.; Mirmoghtadaie, L. Effect of Substitution of Sugar by High Fructose Corn Syrup on the Physicochemical Properties of Bakery and Dairy Products: A Review. *Nutr. Food Sci.* **2016**, *3*, 3–11. [CrossRef]
51. Yadav, A.K.; Singh, S.V. Osmotic dehydration of fruits and vegetables: A review. *J. Food Sci. Technol.* **2014**, *51*, 1654–1673. [CrossRef] [PubMed]
52. Basciano, H.; Federico, L.; Adeli, K. Fructose, insulin resistance, and metabolic dyslipidemia. *Nutr. Metab.* **2005**, *2*, 5. [CrossRef]
53. Bhasin, S.; Modi, H.A. Optimization of Fermentation Medium for the Production of Glucose Isomerase Using *Streptomyces* sp. SB-P1. *Biotechnol. Res. Int.* **2012**, *2012*, 874152. [CrossRef]
54. Serna-Saldivar, S.O. Maize: Foods from Maize. In *Reference Module in Food Science*; Elsevier: Amsterdam, The Netherlands, 2016. [CrossRef]
55. Liu, Z.Q.; Zheng, W.; Huang, J.F.; Jin, L.Q.; Jia, D.X.; Zhou, H.Y.; Xu, J.M.; Liao, C.J.; Cheng, X.P.; Mao, B.X.; et al. Improvement and characterization of a hyperthermophilic glucose isomerase from *Thermoanaerobacter ethanolicus* and its application in production of high fructose corn syrup. *J. Ind. Microbiol. Biotechnol.* **2015**, *42*, 1091–1103. [CrossRef]
56. Singh, R.S.; Chauhan, K.; Singh, R.P. Enzymatic Approaches for the Synthesis of High Fructose Syrup. In *Plant Biotechnology: Recent Advancements and Developments*; Springer: Singapore, 2017; pp. 189–211. [CrossRef]
57. Dai, C.; Miao, T.; Hai, J.; Xiao, Y.; Li, Y.; Zhao, J.; Qiu, H.; Xu, B. A Novel Glucose Isomerase from *Caldicellulosiruptor bescii* with Great Potentials in the Production of High-Fructose Corn Syrup. *Biomed Res. Int.* **2020**, *2020*, 1871934. [CrossRef]
58. Brown, S.H.; Sjoholm, C.; Kelly, R.M. Purification and characterization of a highly thermostable glucose isomerase produced by the extremely thermophilic eubacterium, *Thermotoga maritima*. *Biotechnol. Bioeng.* **1993**, *41*, 878–886. [CrossRef]
59. Deng, H.; Chen, S.; Wu, D.; Chen, J.; Wu, J. Heterologous expression and biochemical characterization of glucose isomerase from *Thermobifida fusca*. *Bioprocess Biosyst. Eng.* **2014**, *37*, 1211–1219. [CrossRef] [PubMed]
60. Jia, D.X.; Zhou, L.; Zheng, Y.G. Properties of a novel thermostable glucose isomerase mined from *Thermus oshimai* and its application to preparation of high fructose corn syrup. *Enzym. Microb. Technol.* **2017**, *99*, 1–8. [CrossRef] [PubMed]
61. Vieille, C.; Hess, J.M.; Kelly, R.M.; Zeikus, J.G. xylA cloning and sequencing and biochemical characterization of xylose isomerase from *Thermotoga neapolitana*. *Appl. Environ. Microbiol.* **1995**, *61*, 1867–1875. [CrossRef] [PubMed]
62. Canilha, L.; Kumar Chandel, A.; dos Santos Milessi, T.S.; Fernandes Antunes, F.A.; da Costa Freitas, W.L.; das Gracas Almeida Felipe, M.; da Silva, S.S. Bioconversion of sugarcane biomass into ethanol: An overview about composition, pretreatment methods, detoxification of hydrolysates, enzymatic saccharification, and ethanol fermentation. *J. Biomed. Biotechnol.* **2012**, *2012*, 989572. [CrossRef] [PubMed]
63. Chiang, L.C.; Gong, C.S.; Chen, L.F.; Tsao, G.T. d-Xylulose Fermentation to Ethanol by *Saccharomyces cerevisiae*. *Appl. Environ. Microbiol.* **1981**, *42*, 284–289. [CrossRef]
64. Gong, C.S.; Chen, L.F.; Flickinger, M.C.; Chiang, L.C.; Tsao, G.T. Production of Ethanol from d-Xylose by Using d-Xylose Isomerase and Yeasts. *Appl. Environ. Microbiol.* **1981**, *41*, 430–436. [CrossRef]

65. Ko, J.K.; Um, Y.; Woo, H.M.; Kim, K.H.; Lee, S.M. Ethanol production from lignocellulosic hydrolysates using engineered *Saccharomyces cerevisiae* harboring xylose isomerase-based pathway. *Bioresour. Technol.* **2016**, *209*, 290–296. [CrossRef] [PubMed]
66. Diao, L.; Liu, Y.; Qian, F.; Yang, J.; Jiang, Y.; Yang, S. Construction of fast xylose-fermenting yeast based on industrial ethanol-producing diploid *Saccharomyces cerevisiae* by rational design and adaptive evolution. *BMC Biotechnol.* **2013**, *13*, 110. [CrossRef] [PubMed]
67. Demeke, M.M.; Dietz, H.; Li, Y.; Foulquie-Moreno, M.R.; Mutturi, S.; Deprez, S.; Den Abt, T.; Bonini, B.M.; Liden, G.; Dumortier, F.; et al. Development of a D-xylose fermenting and inhibitor tolerant industrial *Saccharomyces cerevisiae* strain with high performance in lignocellulose hydrolysates using metabolic and evolutionary engineering. *Biotechnol. Biofuels* **2013**, *6*, 89. [CrossRef] [PubMed]
68. Seike, T.; Kobayashi, Y.; Sahara, T.; Ohgiya, S.; Kamagata, Y.; Fujimori, K.E. Molecular evolutionary engineering of xylose isomerase to improve its catalytic activity and performance of micro-aerobic glucose/xylose co-fermentation in *Saccharomyces cerevisiae*. *Biotechnol. Biofuels* **2019**, *12*, 139. [CrossRef]
69. Bracher, J.M.; Martinez-Rodriguez, O.A.; Dekker, W.J.C.; Verhoeven, M.D.; van Maris, A.J.A.; Pronk, J.T. Reassessment of requirements for anaerobic xylose fermentation by engineered, non-evolved *Saccharomyces cerevisiae* strains. *FEMS Yeast Res.* **2019**, *19*, foy104. [CrossRef]
70. Tran Nguyen Hoang, P.; Ko, J.K.; Gong, G.; Um, Y.; Lee, S.M. Genomic and phenotypic characterization of a refactored xylose-utilizing Saccharomyces cerevisiae strain for lignocellulosic biofuel production. *Biotechnol. Biofuels* **2018**, *11*, 268. [CrossRef]
71. Vilela Lde, F.; de Araujo, V.P.; Paredes Rde, S.; Bon, E.P.; Torres, F.A.; Neves, B.C.; Eleutherio, E.C. Enhanced xylose fermentation and ethanol production by engineered *Saccharomyces cerevisiae* strain. *AMB Express* **2015**, *5*, 16. [CrossRef]
72. Tanino, T.; Hotta, A.; Ito, T.; Ishii, J.; Yamada, R.; Hasunuma, T.; Ogino, C.; Ohmura, N.; Ohshima, T.; Kondo, A. Construction of a xylose-metabolizing yeast by genome integration of xylose isomerase gene and investigation of the effect of xylitol on fermentation. *Appl. Microbiol. Biotechnol.* **2010**, *88*, 1215–1221. [CrossRef]
73. Kuyper, M.; Harhangi, H.R.; Stave, A.K.; Winkler, A.A.; Jetten, M.S.; de Laat, W.T.; den Ridder, J.J.; Op den Camp, H.J.; van Dijken, J.P.; Pronk, J.T. High-level functional expression of a fungal xylose isomerase: The key to efficient ethanolic fermentation of xylose by *Saccharomyces cerevisiae*? *FEMS Yeast Res.* **2003**, *4*, 69–78. [CrossRef]
74. Hector, R.E.; Dien, B.S.; Cotta, M.A.; Mertens, J.A. Growth and fermentation of D-xylose by *Saccharomyces cerevisiae* expressing a novel D-xylose isomerase originating from the bacterium *Prevotella ruminicola* TC2-24. *Biotechnol. Biofuels* **2013**, *6*, 84. [CrossRef]
75. Harcus, D.; Dignard, D.; Lepine, G.; Askew, C.; Raymond, M.; Whiteway, M.; Wu, C. Comparative xylose metabolism among the Ascomycetes *C. albicans*, *S. stipitis* and *S. cerevisiae*. *PLoS ONE* **2013**, *8*, e80733. [CrossRef] [PubMed]
76. Aeling, K.A.; Salmon, K.A.; Laplaza, J.M.; Li, L.; Headman, J.R.; Hutagalung, A.H.; Picataggio, S. Co-fermentation of xylose and cellobiose by an engineered *Saccharomyces cerevisiae*. *J. Ind. Microbiol. Biotechnol.* **2012**, *39*, 1597–1604. [CrossRef] [PubMed]
77. Waltman, M.J.; Yang, Z.K.; Langan, P.; Graham, D.E.; Kovalevsky, A. Engineering acidic *Streptomyces rubiginosus* D-xylose isomerase by rational enzyme design. *Protein Eng. Des. Sel.* **2014**, *27*, 59–64. [CrossRef] [PubMed]
78. Lee, S.M.; Jellison, T.; Alper, H.S. Directed evolution of xylose isomerase for improved xylose catabolism and fermentation in the yeast *Saccharomyces cerevisiae*. *Appl. Environ. Microbiol.* **2012**, *78*, 5708–5716. [CrossRef] [PubMed]